Eur. Phys. J. C (2021) 81:446
https://doi.org/10.1140/epjc/s10052-021-09262-x

THE EUROPEAN PHYSICAL JOURNAL C

Regular Article - Experimental Physics

Resolving XENON excess with decaying cold dark matter

Shuai Xu[a], **Sibo Zheng**[b]

Department of Physics, Chongqing University, Chongqing 401331, China

Received: 30 March 2021 / Accepted: 18 May 2021 / Published online: 24 May 2021

Abstract We propose a decaying cold dark matter model to explain the excess of electron recoil observed at the XENON1T experiment. In this scenario, the daughter dark matter from the parent dark matter decay easily obtains velocity large enough to saturate the peak of the electron recoil energy around 2.5 keV, and the observed signal rate can be fulfilled by the parent dark matter with a mass of order 10–200 MeV and a lifetime larger than the age of Universe. We verify that this model is consistent with experimental limits from dark matter detections, Cosmic microwave background and large scale structure experiments.

1 Introduction

Recently, XENON1T experiment [1], which is a dark matter (DM) direct detection facility, has reported an excess of electron recoil over the background in the 1–7 keV range with 3.5σ significance. As pointed out in Ref. [1], this excess is unlikely due to solar axion, neutrino magnetic moment or statistical uncertainties about the background. So far, the observed excess has initiated extensive investigations about potential astrophysical sources. Among other things, a cold DM is a natural candidate, which is the subject of this study.

To explain the observed excess, one has to accommodate two critical quantities - the electron recoil energy range around 2–3 keV and the electron transfer momentum range near 50 keV. Unfortunately, they conflict with a conventional cold DM, which has a velocity typically of order $\sim 10^{-3}c$, with c the velocity of light. A few proposals have been proposed to avoid the conflicts. In the case of elastic scattering [2–7], the cold DMs can be boosted in certain circumstances before they interact with the electrons in the xenon atoms, while in the case of inelastic scattering [8–12] the favored electron transfer momentum range can be realized in terms of small rest mass splitting between two different DM components.

In this study, we propose a new decaying cold DM scenario, in which the parent DM (A) decays to the daughter DM particles (B),

$$A \to BB. \tag{1}$$

In terms of the decay, the velocity of the daughter DM can be enhanced to be comparable with c, relative to the small velocity of the parent DM. Unlike photoelectric absorption in a decaying warm DM [13], the daughter particle elastically scatters off the electrons in the xenon atoms. We will show that without any violations of current DM (in)direct detections or cosmological measurements, this decaying cold DM model can easily resolve the XENON excess.

2 The model

We begin with the production of the daughter particle B due to A decay. The decay yields the following velocity and present number density of B respectively,

$$\frac{\upsilon_B}{c} = \sqrt{\frac{m_A^2}{4m_B^2} - 1}, \tag{2}$$

$$n_B = 2\frac{\rho_{\rm dm,0}}{m_A}\left[1 - \exp\left(-\Gamma_A \mathrm{t}_0\right)\right], \tag{3}$$

where m_A and m_B refer to the parent and daughter DM mass respectively with $m_A > 2m_B$, t_0 is the age of Universe, while $\rho_{\rm dm,0} = 0.4\ \mathrm{GeV/cm^3}$ and Γ_A denote the local DM density and the decay width of the parent DM A, respectively. We will assume that compared to the decay production the thermal production of n_B is subdominant.

The input parameters in Eqs. (2) and (3) are constrained as follows. Firstly, in order to yield υ_B of order $\sim 0.1\ c$ the mass ratio $m_A/2m_B$ should deviate from unity in percent level, which implies that m_A and $2m_B$ are highly degenerate.

[a] e-mail: shuaixu@cqu.edu.cn

[b] e-mail: sibozheng.zju@gmail.com (corresponding author)

Secondly, in order to fulfill the cosmological bounds on the decaying DM both from the Cosmic microwave background (CMB) and large scale structure (LSS) experiments, the lifetime of A particle $\tau_A = \Gamma_A^{-1}$ should be larger than t_0, which can be achieved by adjusting the coupling constant between A and B, with the help of a suppression by the small β factor due to the mass degeneracy.

We will return to the cosmological constraints after we have explored the signal rate of the recoil electrons at the XENON1T.

3 Signal rate

According to conservations of energy and momentum in the elastic scattering process, the energy[1] transferred to electron reads [14]

$$E_e = \mathbf{q} \cdot \vec{\upsilon}_B - \frac{q^2}{2m_B}. \tag{4}$$

From Eq. (4) the maximal value $E_e^{\max} \approx \frac{1}{2} m_B \upsilon_B^2$ at $q \approx m_B \upsilon_B$ valid only when $m_B \approx m_e$. Consider that when $m_B \leq m_e$ the daughter DM with a large velocity is severely constrained by limits such as the effective number of neutrinos, we will focus on $m_B \gg m_e$, under which $E_e^{\max} \approx 2 m_e \upsilon_B^2$ [2] instead. This constraint implies $\upsilon_B \geq 0.05\, c$ in order to satisfy $E_e^{\max} \geq 2.5$ keV.

Given a fixed value of E_e, Eq. (4) determines the electron transfer momentum range $q_- < q < q_+$, with

$$q_\pm = m_B \upsilon_B \pm \sqrt{m_B^2 \upsilon_B^2 - 2 m_B E_e}. \tag{5}$$

The transfer momentum range in Eq. (5) affects the signal rate of the recoil electrons discussed below in the sense that the atomic factorization factor $K(E_e, q)$ [15,16] is rather sensitive to q, which takes the maximal value $K_{\max} \approx 0.1$ at $q_{\text{peak}} \approx 50$ keV for $E_e = 2$ keV, and dramatically declines as q slightly deviates from q_{peak}. Therefore, in order to maximize the K-factor contribution to the signal rate, we should take suitable values of m_B and υ_B to make sure that q_{peak} is covered by the electron transfer momentum range in Eq. (5).

Furthermore, the daughter DM-free electron scattering cross section $\bar{\sigma}_e$ relies on the nature of mediator [17] which communicates the interaction between the daughter DM B and electron. From the viewpoint of effective field theory, $\bar{\sigma}_e$ can be written as

$$\bar{\sigma}_e \approx \frac{g_{mB}^2 g_{me}^2 m_e^2}{\pi m_{\text{med}}^4}, \tag{6}$$

[1] In the case of inelastic scattering, E_e in Eq. (4) receives a new term due to the rest mass splitting between two different components that involve in the scattering off electron.

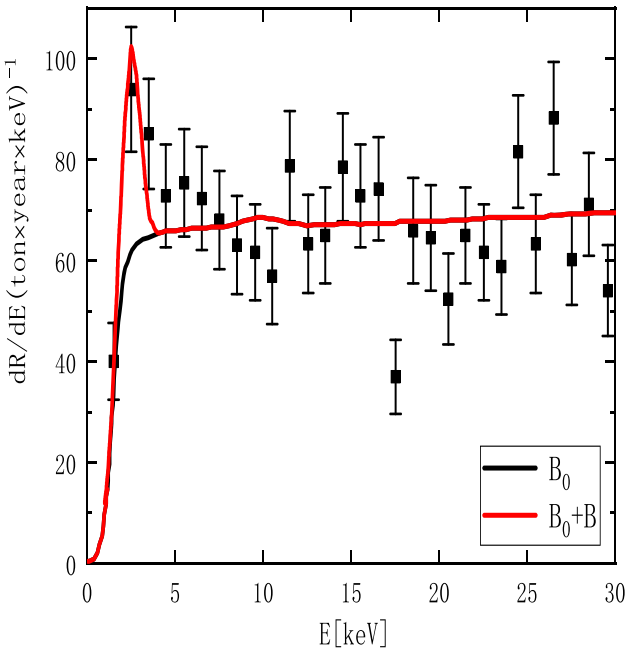

Fig. 1 Fit to the observed data [1] about the number of events dR/dE (ton year keV)$^{-1}$ as function of the reconstructed electron recoil energy with five different sets of benchmark values C1 to C5 in Table 1, where B_0 and B represents the background and the daughter DM contribution, respectively

where m_{med} is the mediator mass, g_{mB} is the coupling between the mediator and B, and g_{me} is the coupling between the mediator and electron. If the mediator is identified as a standard model particle, only g_{mB} in Eq. (6) is a free parameter, the magnitude of which has to be constrained by the decay width of the standard model particle.

After a handle on the "luminosity" and the DM B-electron scattering cross section, we now estimate the number of events of recoil electrons

$$\frac{dR}{dE} \approx n_{\text{xe}} n_B \times \frac{\bar{\sigma}_e}{2 m_e \upsilon_B} \times \int dE_e \left[\int_{q_-}^{q_+} dq a_0^2 q \mid F(q) \mid^2 K(E_e, q) \right] R_s(E, E_e), \tag{7}$$

where $n_{\text{xe}} \approx 4.2 \times 10^{27}$/ton is the number density of xenon atoms in the detector, $a_0 = 1/(\alpha_{\text{em}} m_e)$ is the Bohr radius with $\alpha_{\text{em}} = 1/137$, $F(q) \approx 1$ is the DM form factor, and R_s is the resolution function which accounts for the "efficiency" of the detector. We will simply take the Gaussian distribution for the reconstructed energy for numerical analysis

$$R_s(E, E_e) = \frac{\alpha(E)}{\sqrt{2\pi}\sigma} \exp\left[-\frac{(E - E_e)^2}{2\sigma^2} \right], \tag{8}$$

where $\alpha(E)$ is the efficiency [1] and $\sigma = a\sqrt{E_e} + b E_e$, with $a = (0.310 \pm 0.004)\ \sqrt{\text{keV}}$ and $b = 0.0037 \pm 0.0003$, respectively.

Table 1 Five sets of benchmark values which yield the same fit as shown in Fig. 1, where the required values of $\bar{\sigma}_e$ can be understood as an output parameter

	m_A (MeV)	m_B(MeV)	υ_B/c	τ_A/t_0	$\bar{\sigma}_e$ (cm^2)
C1	10.05	5	0.1	3	4.36×10^{-45}
C2	20.1	10	0.1	3	9.46×10^{-45}
C3	40.2	20	0.1	3	1.89×10^{-44}
C4	100.5	50	0.1	3	4.22×10^{-44}
C5	201	100	0.1	3	8.06×10^{-44}

Figure 1 shows the fit to the reported XENON1T data [1] with five different sets of benchmark values C1 to C5 as explicitly shown in Table 1. In individual case therein, we have chosen fixed value $\tau_A = 3\ \mathrm{t}_0$, under which $m_A \approx 2m_B$ take the mass ranges of $10 - 200$ MeV and $\upsilon_B/c = 0.1$. The values of $\bar{\sigma}_e$ inferred from the observed XENON excess varies from $\mathcal{O}(10^{-45})$ cm^2 to $\mathcal{O}(10^{-44})$ cm^2.

4 Dark matter constraints

Now we turn to possible constraints on the dark matter particles A and B. Since the interaction in Eq. (1) yields too small annihilation cross section for A to accommodate the required thermal annihilation cross section, A has to communicate either with the Standard Model (SM) sector e.g. via the same mediator as B, or mainly with other unstable freedoms in the dark sector. In the former situation, some constraints on B as below can be placed on A as well.

With the communication between B and the SM sector as inferred from the XENON1T excess, we can at least place the following constraints.

- The daughter DM B-free electron scattering cross section $\bar{\sigma}_e$, extracted from the XENON1T excess, can be used to constrain the model parameters. Based on the measurements on $\bar{\sigma}_e$ within various electron recoil energies, the light daughter DM can be probed either by the current XENON1T [18,19] or the future SuperCDMS [20] experiments.

- Similar to the DM B-electron scattering, we can also constrain m_B from the annihilation cross section $\sigma^B_{\mathrm{ann}}(BB \to e^+e^-)$, based on the cross symmetry between the two Feynman diagrams related to these two processes. While experiments such as AMS-01 [21], AMS-02 [22] or PAMELA [23] have not yet placed viable bounds on σ^B_{ann} in the sub GeV-scale DM mass, the Planck data [24] is able to constrain m_B down to ~ 1 MeV.

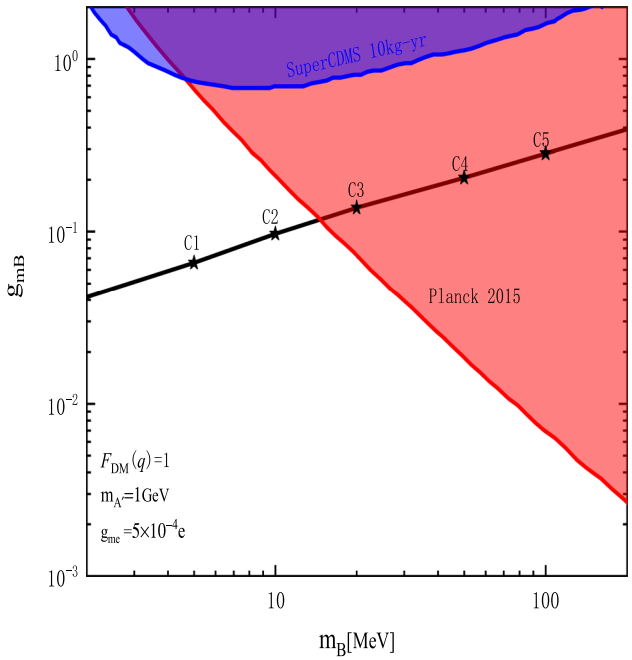

Fig. 2 Constraints on the parameter space (in black curve) in the dark photon model with $m_{A'} = 1$ GeV, $g_{me} = 5 \times 10^{-4}e$ and the DM form factor $F(q) = 1$. We have simultaneously shown the SuperCDMS limit [20] (in blue) and the Planck 2015 limit [27] (in red), where the shaded regions are excluded

- Lastly, the coupling of the mediator to electron can be constrained by colliders such as BaBar, LEP and LHC.

For illustration, we show in Fig. 2 the constraints in the specific dark photon model with the mediator identified as a new vector boson A', where $m_{A'} = 1$ GeV and $g_{me} = 5 \times 10^{-4}e$ have been adopted in the light of BaBar data [25]. In this figure, we have simultaneously shown the SuperCDMS limit [20] (in blue) without relativistic effect [26], the Planck 2015 limit [27] (in red) and the parameter space (in black curve) together with the benchmark values in Table 1. Relatively weaker XENON1T limit has been ignored. One observes that in this explicit model m_B beneath ~ 15 MeV survives.

Compared to the benchmark values in Table 1, given fixed m_B one can obtain larger $\bar{\sigma}_e$ or alternatively larger $g_{mB}g_{me}$ by taking larger τ_A, since they are linearly correlated to each other in $dR/dE \sim \bar{\sigma}_e(t_0/\tau_A)$ for $t_0 \ll \tau_A$ in Eq. (7). However, an increase of τ_A will simultaneously lead to linearly enhanced experimental limits in Fig. 2. These trends together imply that adjusting τ_A is unable to alter the SuperCDMS sensitivity as illustrated in Fig. 2.

5 Cosmological constraints

The decaying DM model are constrained both by the CMB and the LSS experiments for a varying dark matter energy density with time. In our scenario, it reads from Eq. (3)

$$\rho_{\rm dm}(t) = \rho_{\rm dm,0}\left[e^{-t/\tau_A} + \frac{2m_B}{m_A}\left(1 - e^{-t/\tau_A}\right)\right]a^{-3}(t), \tag{9}$$

Compared to the baseline ΛCDM cosmology, the DM relic density in Eq. (9) is altered by a magnitude of order $|\Delta\rho_{\rm dm}/\rho_{\rm dm,0}| \approx (1 - \frac{2m_B}{m_A})t/\tau_A < 10^{-3}$ in the small redshift region for the benchmark values in Table 1, as a result of highly degenerate dark matter mass relation $m_A \approx 2m_B$ required by the XENON excess.

For the CMB experiment [28], it mainly affects the temperature power spectrum C_{TT} in terms of the integrated Sachs-Wolfe effect, which relies on the cosmological evolution of Universe after the last scattering. Due to the small fraction in $\rho_{\rm dm}$ given by Eq. (9) relative to what attempts to explain the Hubble tension [29–32], the effect on C_{TT} in our scenario is negligible. For the LSS experiments, the DM power spectrum $\delta = \delta\rho_{\rm dm}/\rho_{\rm dm}$ evolves with time as

$$\ddot{\delta} + 2H\dot{\delta} - 4\pi G\rho_{\rm dm}\delta = 0, \tag{10}$$

where G is the Newton's constant and H is the Hubble rate. The small fraction in $\rho_{\rm dm}$ gives rise to a fraction in the DM power spectrum δ less than the order of a percent level, which is far beyond the reach of future LSS experiments such as the Dark Energy Spectroscopic Instrument [33].

6 Conclusions

In this study we have proposed a novel decaying cold DM scenario in which the cold parent DM A decays to the daughter particle B, with the lifetime τ_A larger than the age of Universe. Firstly we have shown that in this scenario the observed excess of the electron recoil at the XENON1T in the energy range 2–3 keV can be addressed by the daughter DM B-electron elastic scattering with the DM mass ranges $m_A \approx 2m_B \sim$ 10–200 MeV. Moreover, we have verified that because of small DM B-electron scattering cross section this model is consistent with limits both from the DM direct and indirect detections, while as a result of suppression on the magnitude of the fraction in the DM energy density due to the highly degenerate mass relation imposed by the XENON excess, this model does not violate either the CMB measurements on the temperature power spectrum or the LSS constraints on the DM power spectrum. Finally, there are a few directions in our DM scenario which deserve further investigation. Especially, if we are allowed to adopt the lifetime of the parent DM obviously smaller than the age of Universe, it is not unlikely to resolve the XENON1T excess and the Hubble tension simultaneously with a decaying cold DM.

Acknowledgements The research is supported in part by the National Natural Science Foundation of China with Grant no. 11775039 and the Fundamental Research Funds for the Central Universities at Chongqing University with Grant no. cqu2017hbrc1B05.

Data Availability Statement This manuscript has no associated data or the data will not be deposited. [Authors' comment: All data has been included in the table and figures.]

Funded by SCOAP[3].

References

1. E. Aprile et al. [XENON], Excess electronic recoil events in XENON1T. Phys. Rev. D **102**(7), 072004 (2020). arXiv:2006.09721 [hep-ex]
2. K. Kannike, M. Raidal, H. Veermäe, A. Strumia, D. Teresi, Dark matter and the XENON1T electron recoil excess. Phys. Rev. D **102**(9), 095002 (2020). arXiv:2006.10735 [hep-ph]
3. B. Fornal, P. Sandick, J. Shu, M. Su, Y. Zhao, Boosted dark matter interpretation of the XENON1T excess. Phys. Rev. Lett. **125**(16), 161804 (2020). arXiv:2006.11264 [hep-ph]
4. L. Su, W. Wang, L. Wu, J.M. Yang, B. Zhu, Atmospheric Dark Matter and Xenon1T Excess. arXiv:2006.11837 [hep-ph]
5. N.F. Bell, J.B. Dent, B. Dutta, S. Ghosh, J. Kumar, J.L. Newstead, Explaining the XENON1T excess with luminous dark matter. Phys. Rev. Lett. **125**(16), 161803 (2020). arXiv:2006.12461 [hep-ph]
6. Q.H. Cao, R. Ding, Q.F. Xiang, Exploring for sub-MeV boosted dark matter from Xenon electron direct detection. arXiv:2006.12767 [hep-ph]
7. Y. Jho, J.C. Park, S.C. Park, P.Y. Tseng, Leptonic new force and Cosmic-ray boosted dark matter for the XENON1T excess. Phys. Lett. B **811**, 135863 (2020). arXiv:2006.13910 [hep-ph]

8. K. Harigaya, Y. Nakai, M. Suzuki, Inelastic dark matter electron scattering and the XENON1T excess. Phys. Lett. B **809**, 135729 (2020). arXiv:2006.11938 [hep-ph]
9. J. Bramante, N. Song, Electric but not eclectic: thermal relic dark matter for the XENON1T excess. Phys. Rev. Lett. **125**(16), 161805 (2020). arXiv:2006.14089 [hep-ph]
10. A. Aboubrahim, M. Klasen, P. Nath, Xenon-1T excess as a possible signal of a sub-GeV hidden sector dark matter. arXiv:2011.08053 [hep-ph]
11. H.M. Lee, Exothermic dark matter for XENON1T excess. arXiv:2006.13183 [hep-ph]
12. M. Baryakhtar, A. Berlin, H. Liu, N. Weiner, Electromagnetic signals of inelastic dark matter scattering. arXiv:2006.13918 [hep-ph]
13. G. Choi, M. Suzuki, T.T. Yanagida, Phys. Lett. B **811**, 135976 (2020). arXiv:2006.12348 [hep-ph]
14. I.M. Bloch, A. Caputo, R. Essig, D. Redigolo, M. Sholapurkar, T. Volansky, Exploring new physics with O(keV) electron recoils in direct detection experiments. arXiv:2006.14521 [hep-ph]
15. B.M. Roberts, V.V. Flambaum, Electron-interacting dark matter: implications from DAMA/LIBRA-phase2 and prospects for liquid xenon detectors and NaI detectors. Phys. Rev. D **100**(6), 063017 (2019). arXiv:1904.07127 [hep-ph]
16. B.M. Roberts, V.A. Dzuba, V.V. Flambaum, M. Pospelov, Y.V. Stadnik, Dark matter scattering on electrons: accurate calculations of atomic excitations and implications for the DAMA signal. Phys. Rev. D **93**(11), 115037 (2016). arXiv:1604.04559 [hep-ph]
17. H. Alhazmi, D. Kim, K. Kong, G. Mohlabeng, J.C. Park, S. Shin, Implications of the XENON1T excess on the dark matter interpretation. arXiv:2006.16252 [hep-ph]
18. E. Aprile et al. [XENON], Phys. Rev. Lett. **123**(25), 251801 (2019). arXiv:1907.11485 [hep-ex]
19. R. Essig, T. Volansky, T.T. Yu, New constraints and prospects for sub-GeV dark matter scattering off electrons in Xenon. Phys. Rev. D **96**(4), 043017 (2017). arXiv:1703.00910 [hep-ph]
20. R. Essig, M. Fernandez-Serra, J. Mardon, A. Soto, T. Volansky, T.T. Yu, Direct detection of sub-GeV dark matter with semiconductor targets. JHEP **05**, 046 (2016). arXiv:1509.01598 [hep-ph]
21. M. Aguilar et al. [AMS 01], Cosmic-ray positron fraction measurement from 1 to 30-GeV with AMS-01. Phys. Lett. B **646**, 145–154 (2007). arXiv:astro-ph/0703154
22. M. Aguilar et al. [AMS], First result from the alpha magnetic spectrometer on the international space station: precision measurement of the positron fraction in primary Cosmic rays of 0.5–350 GeV. Phys. Rev. Lett. **110**, 141102 (2013)
23. O. Adriani et al., [PAMELA], Cosmic-ray positron energy spectrum measured by PAMELA. Phys. Rev. Lett. **111**, 081102 (2013). arXiv:1308.0133 [astro-ph.HE]
24. P.A.R. Ade et al. [Planck], Planck 2015 results. XIII. Cosmological parameters. Astron. Astrophys. **594**, A13 (2016). arXiv:1502.01589 [astro-ph.CO]
25. J.P. Lees et al. [BaBar], Search for a Dark Photon in e^+e^- Collisions at BaBar. Phys. Rev. Lett. **113**(20), 201801 (2014). arXiv:1406.2980 [hep-ex]
26. M.K. Pandey, L. Singh, C.P. Wu, J.W. Chen, H.C. Chi, C.C. Hsieh, C.P. Liu, H.T. Wong, Constraints on spin-independent dark matter scattering off electrons with germanium and xenon detectors. arXiv:1812.11759 [hep-ph]
27. T.R. Slatyer, Indirect dark matter signatures in the cosmic dark ages. I. Generalizing the bound on s-wave dark matter annihilation from Planck results. Phys. Rev. D **93**(2), 023527 (2016). arXiv:1506.03811 [hep-ph]
28. N. Aghanim et al. [Planck], Planck 2018 results. VI. Cosmological parameters. Astron. Astrophys. **641**, A6 (2020). arXiv:1807.06209 [astro-ph.CO]
29. K. Vattis, S.M. Koushiappas, A. Loeb, Dark matter decaying in the late Universe can relieve the H0 tension. Phys. Rev. D **99**(12), 121302 (2019). arXiv:1903.06220 [astro-ph.CO]
30. L.A. Anchordoqui, V. Barger, H. Goldberg, X. Huang, D. Marfatia, L.H.M. da Silva, T.J. Weiler, IceCube neutrinos, decaying dark matter, and the Hubble constant. Phys. Rev. D **92**(6), 061301 (2015). arXiv:1506.08788 [hep-ph]
31. T. Bringmann, F. Kahlhoefer, K. Schmidt-Hoberg, P. Walia, Converting nonrelativistic dark matter to radiation. Phys. Rev. D **98**(2), 023543 (2018). arXiv:1803.03644 [astro-ph.CO]
32. S.J. Clark, K. Vattis, S.M. Koushiappas, CMB constraints on late-universe decaying dark matter as a solution to the H_0 tension. arXiv:2006.03678 [astro-ph.CO]
33. A. Aghamousa et al. [DESI], The DESI experiment part I: science,targeting, and survey design. arXiv:1611.00036 [astro-ph.IM]